Supplementary File

Detection of dietary stress and geophagic behaviour forced by dry seasons in Miocene *Gomphotherium*

(see https://doi.org/10.5281/zenodo.14882824 for further information)

1. Elemental data processing

To ensure only enamel data was included in the main dataset and that potential alteration was excluded from (paleo)environmental analysis, a series of steps were followed, as described in the sequence below:

Step 1. Raw data obtained via µXRF was calibrated to eliminate matrix effects on the elemental composition result This calibration consists of a two-step process in which XRF spectra were first quantified in the Bruker Esprit software through a one-standard quantification routine to remove the matrix effect. The standard used for this quantification step was the BAS CRM 393 limestone standard from the Bureau of Analyzed Samples (Middlesborough, UK; see also de Winter and Claeys, 2016). In a second step, the quantified data was calibrated using a set of 10 carbonate standards that were quantified using the same routine (see Vellekoop et al., 2022).

Step 2. After this step, a filter was applied to ensure only apatite measurements were included in the dataset, which significantly reduces "noise" from cracks, measurements at the edges of the samples, dirt speckles. This filter consisted in selecting measurements with a range of Ca and P characteristic for enamel apatite (Ca concentrations >330000 ppm; P concentrations >150000 ppm). By doing this, most diagenetic features will also be excluded from the original dataset, as calcium is replaced by other elements during late/burial diagenetic processes (see main text).

Step3. Calcium normalization of selected elements (Fe, Al, Na and Si) was tested in order to confirm if elemental trends could be affected by fluctuations in Ca content (Fig. S1). A very significant positive linear correlation was obtained between absolute and calcium-corrected elemental values, in all cases Pearson's $r>0.99$ (Fig. S1). Since no differences are detected between both datasets, the use of absolute elemental data is preferred (see main text for discussion).

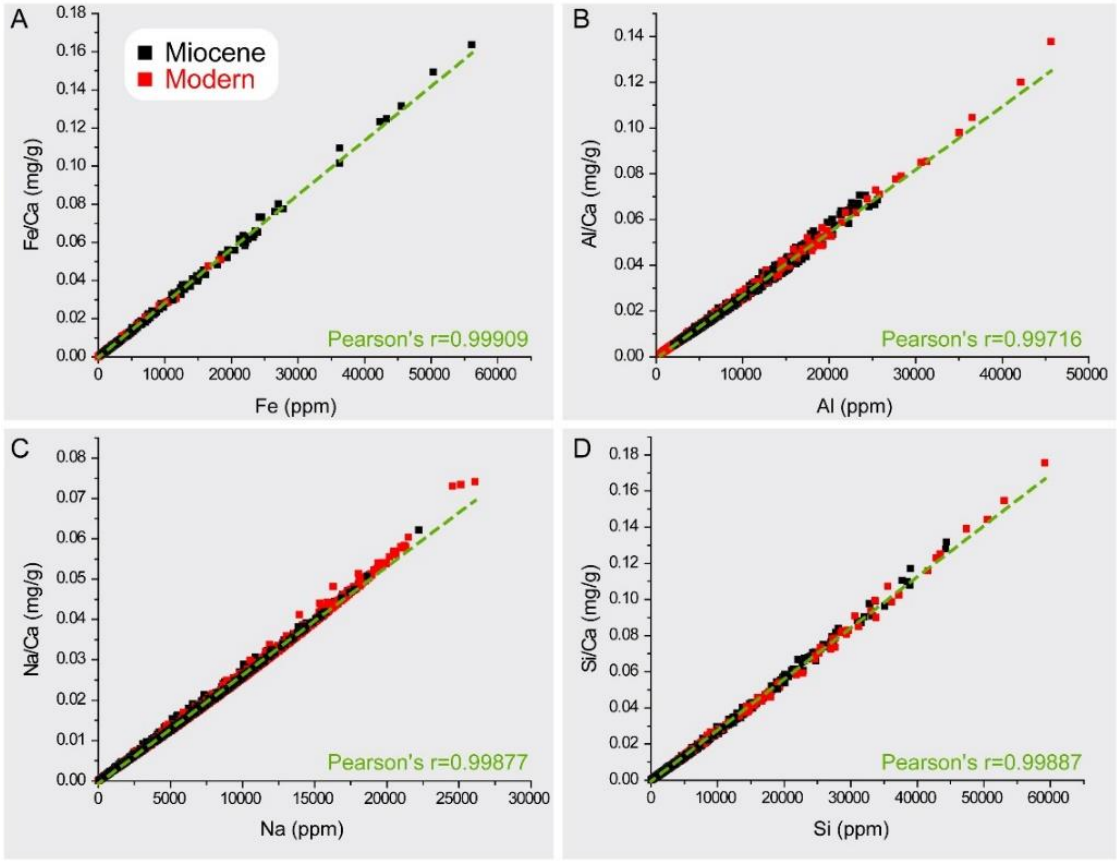

Fig. S1. Comparison between absolute and Ca-corrected values. A) to D) Scatter plot and respective linear correlation for absolute values (ppm) and calcium-corrected (element/Ca) for Fe, Al, Na and Si abundance. Note highly significant correlation (R>0.99) for all tested elements.

Step 4. Only data considered valid are present in our dataset and "noise" is extremely reduced. Consequently, a high number of empty cells is verified in some measured elements, limiting the representativity of statistical analysis performed to the dataset. In these cases, empty cells were replaced by the mean value of that given proxy along the measured transect. All statistic procedures were performed before and after this replacement, ensuring that no changes occurred (as expected). Statistical analysis including comparisons between different elements (Principal Component Analysis-PCA) saw pairing improved from 8% to 100% for Mid-Miocene samples and from 68% to 100% for modern molar samples (see Fig. 7 of the main text for PCA results after mean value replacement).

Step 5. Given the elemental clusters obtained via PCA, among which Fe plays an important role (Fig. 6 of the main text), there was a possibility that despite prior data-cleaning, evidence of diagenesis could still be present in the dataset. This because Fe enrichment can be used as diagnostic element for diagenetic alteration in ancient proboscidean enamel (Białas et al., 2021). A diagenesis-detection protocol was therefore applied, the "double PCA+" approach consisting of two consecutive PCAs with intermediate steps assisted by density analysis (Coimbra et al., 2017; Coimbra et al., 2020). Very incomplete elemental records (N<30% of total measured points) are

here not considered of relevance, as is the case of Mn and S in the modern molar record (see Fig. 6 of the main text). Scores of the first PCA were used for density analysis (Fig. S2) and only samples included within the range of higher density cluster (main cluster) were selected for performing the second PCA. The goal was to exclude samples spreading away from the main cluster, potentially caused by elemental enrichment during diagenetic alteration.

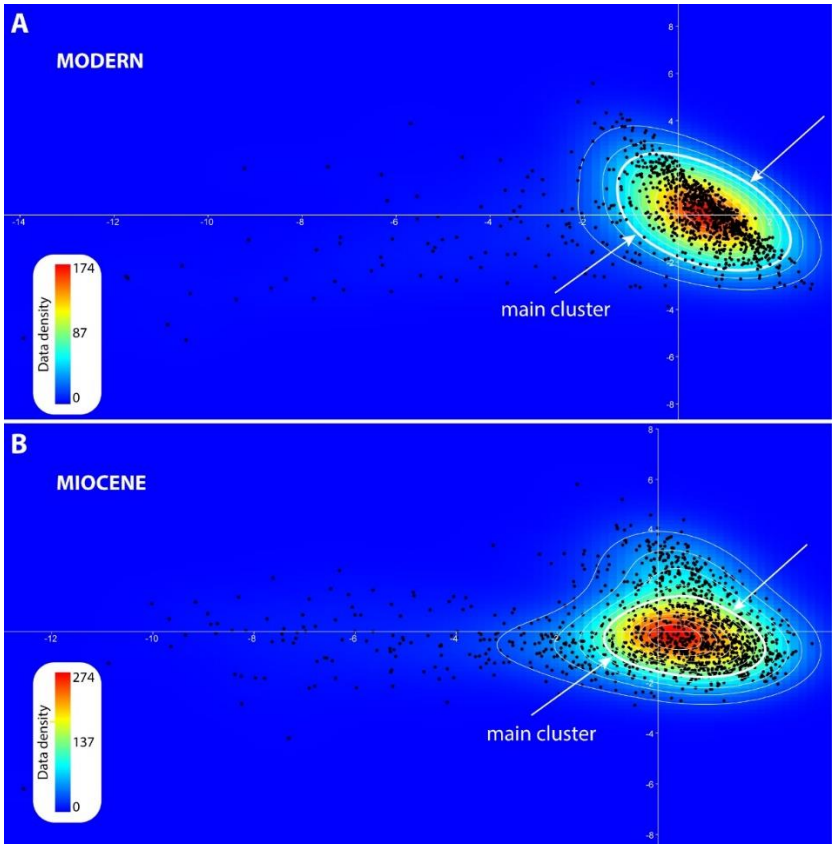

Fig. S2. Principal Component Analysis scores evaluated by density analysis. A) Main cluster for modern molar samples indicated with a bold line (and arrows); B) Main cluster for Mid-Miocene molar samples indicated by bold line (and arrows). Note that the main cluster is defined by densities >1/3 (green to red hues) and undistorted contour lines (white lines marked with arrows).

The now "clean dataset" was used to perform the second PCA (Fig. S3), revealing a complete detrending of the elemental associations previously detected (Fig. S3A and B, compare to results shown in Fig. 6 of the main text) and the distribution of the samples became totally random, without any particular cluster of samples (Fig. S3C and D). The resulting "clean dataset" could therefore correspond to the (paleo)environmental background information, free of syn to post-depositional alteration.

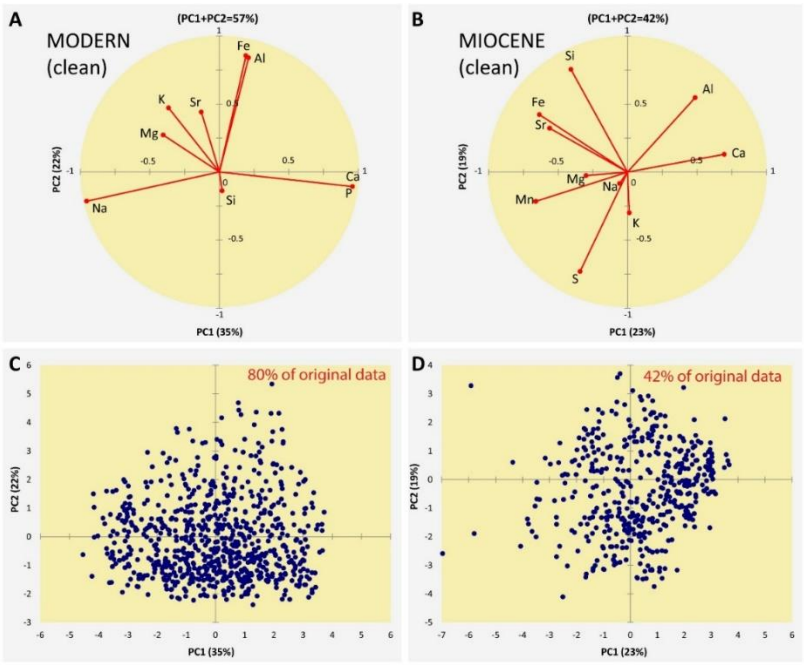

Fig. S3. Second PCA results performed to the "clean dataset". A and B) PCA loadings showing the decoupling of selected elemental variables. C and D) PCA scores for samples representing 80% of the modern dataset and 42% the Mid-Miocene dataset (100% is considered after replacing mean values, see Step 4). Note the lack of clustering in sample distribution.

Step 6. Raw and "clean" datasets were compared in terms of their elemental trends along the measured lines (Fig. S4).

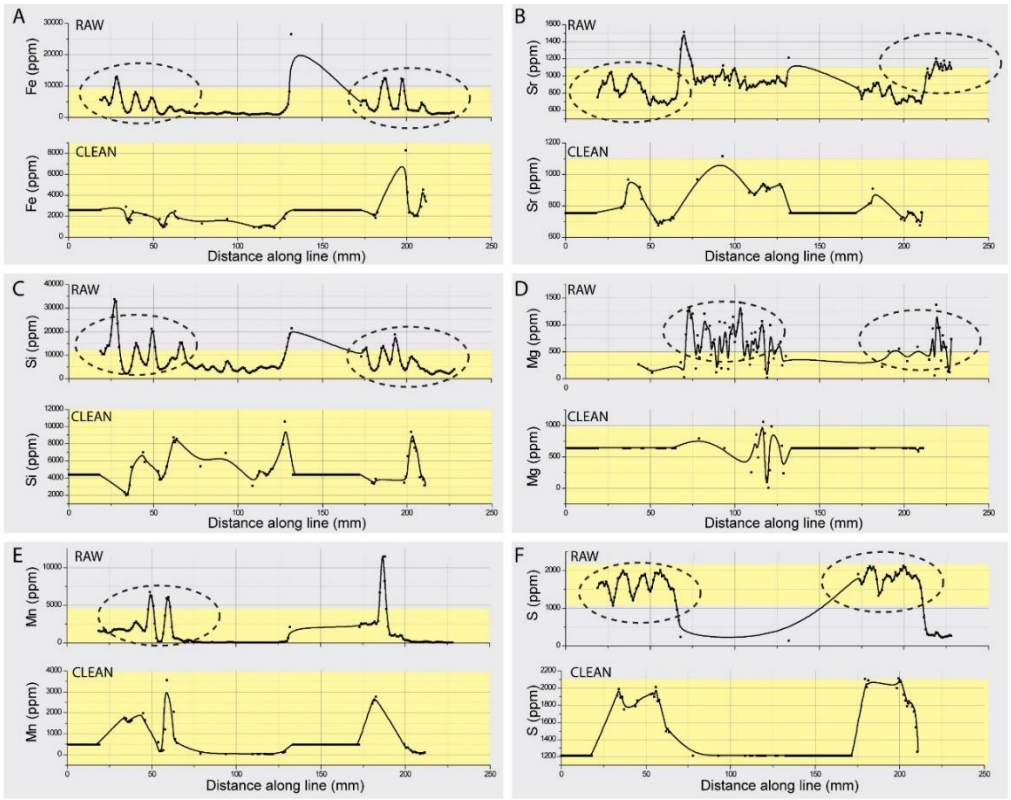

Fig. S4. Examples of comparison between raw data transects and obtained profiles after data cleaning process (dashed lines signal relevant trends in raw data which are eliminated during data processing). More data available at https://doi.org/10.5281/zenodo.14882824.

The elemental fluctuations detected along portions of the raw dataset were obliterated during the Double PCA+ procedure (Fig. S4), resulting in elemental transects that are largely unchanged during molar growth. The deduction based on the results of this procedure is that initial elemental trends are in fact the reflection of environmental controls on elemental incorporation during teeth growth. Based on the previous, the best record of (paleo) environmental fluctuation during the time interval when the molar under scope developed is enclosed within the initial (pre-cleaning) dataset. This is therefore the dataset used throughout the main text (Figs. 9 to 13).

Table S1. Scaling factors used in Figures 11 and 12. Grey cells indicate no change regarding original line length (see main text for details).

	Sample	Direction	Scaling Factors					
Line transects Fe (ppm)			line1	line2	line3	line4	line5	line6
	4944, 4943	horiz.	4.9	4.1	4.2	7.1	7.7	9.3
		vert.	1	1	1	1	9.7	5.5
			line1	line2	line3			
	4945	horiz.	5.1	3.2	3.5			
		vert.	6.2	1	2.3			
			line 1,2		lines3,4		lines5,6	lines7,8,9
	4946	horiz.	4.9		4.4		3.7	3.2
		vert.	3.9		1		8.8	1
Line transects Na (ppm)			line1	line2	line3	line4	line5	line6
	4944, 4943	horiz.	4.9	4.1	4.2	7.1	7.7	9.3
		vert.	1	1	1	1	1	1
			line1	line2	line3			
	4945	horiz.	5.1	3.2	3.5			
		vert.	1	1	1			
			line 1,2		lines3,4		lines5,6	lines7,8,9
	4946	horiz.	4.9		4.4		3.7	3.2
		vert.	1		1		1	1

References:

Coimbra, R., Horikx, M., Huck, S., Heimhofer, U., Immenhauser, A., Rocha, F., Dinis, J., Duarte, L.V., 2017. Statistical evaluation of elemental concentrations in shallow-marine deposits (Cretaceous, Lusitanian Basin). Marine and Petroleum Geology 86, 1029-1046.

Coimbra, R., Huck, S., de Winter, N.J., Heimhofer, U., Claeys, P., 2020. Improving the detection of shell alteration: Implications for sclerochronology. Palaeogeography, Palaeoclimatology, Palaeoecology, 109968.

de Winter NJ, Claeys P. 2016. Micro X-ray fluorescence (μXRF) line scanning on Cretaceous rudist bivalves: A new method for reproducible trace element profiles in bivalve calcite. Petrizzo MR, editor. Sedimentology 64: 231–251. doi:10.1111/sed.12299

Vellekoop J, Kaskes P, Sinnesael M, Huygh J, Déhais T, Jagt JWM, et al. (2022). A new age model and chemostratigraphic framework for the Maastrichtian type area (southeastern Netherlands, northeastern Belgium). nos. 55: 479–501. doi:10.1127/nos/2022/0703